JOURNAL OF APPLIED ELECTROCHEMISTRY **27** (1997) 428–433

Preparation of highly dispersed gold microparticles and their electrocatalytic activity for the oxidation of formaldehyde

H. YANG, T. H. LU*

Changchun Institute of Applied Chemistry, Chinese Academy of Sciences, Changchun 130022, P. R. China

K. H. XUE

Department of Chemistry, Nanjing Normal University, Nanjing 210097, P. R. China

S. G. SUN, S. P. CHEN

Department of Chemistry, Xiamen University, Xiamen 361005, P. R. China

Received 15 April 1996; revised 24 July 1996

The electrochemical preparation of highly dispersed Au microparticles on the surfaces of glassy carbon (GC) electrodes and their electrocatalytic activities for the oxidation of formaldehyde were studied. It was found that the reduction of Au^{3+} to Au is controlled by diffusion and the formation mechanism of Au microparticles on the GC surfaces corresponds to an instantaneous nucleation and diffusion-controlled three dimensional growth process. The particle size is about 80–90 nm in diameter after the electrochemical ageing treatment. These highly dispersed Au microparticles have high surface areas and exhibit better electrocatalytic activity than that of bulk-form Au toward the electrochemical oxidation of formaldehyde in alkaline media.

1. Introduction

The oxidation of small organic molecules at precious metal (e.g. Pt, Pd, Au) electrodes has been extensively investigated. Systems with highly dispersed metal microparticles provide the large surface areas and low coordination atoms necessary for efficient catalysis. Highly dispersed metal microparticles (e.g. Pt, Pd, Au, Cu) may be prepared by many methods [1–8], among which the direct electrochemical reduction of metal ions on an electrode surface is one method. The electrochemical dispersion mechanism and the surface structure and electrocatalytic characteristics of Pt microparticles deposited on surfaces of GC electrodes have been reported [1–3]. Yahikozawa *et al.* [7, 9] have studied the electrocatalytic properties of Au microparticles prepared by vaccum evaporation for the oxidation of formaldehyde. However, the preparation of electrochemical dispersed Au microparticles and their electrocatalytic properties have not been reported.

Gold exhibits electrocatalytic activity in the oxidation of formaldehyde [10–14] and carbon monoxide [15, 16] in alkaline media. To improve the electrocatalytic performance and reduce the amount of gold used, the electrochemical dispersion of the microparticles deposited on the surfaces of the GC electrodes were studied and the electrocatalytic activities of the Au microparticles with a diameter of few tens of nanometres in the oxidation of formaldehyde in alkaline media were evaluated.

2. Experimental details

The chemicals were all of reagent grade. Paraformaldehyde was refluxed for 4 h to obtain pure formaldehyde and verified with FTIR spectroscopy. Solutions were prepared with triple distilled water.

Electrochemical measurements were performed using a model 273 potentiostat/galvonostat (EG&G, PAR Co., USA), Lz3-204 X–Y recorder (Shanghai no.2 Instrument Ltd, China) and a conventional three-electrode electrochemical cell. The working electrode was GC, Au or Au/GC electrode (a GC electrode modified with Au microparticles). The exposed apparent area was approximately 6.88 mm^2 for the GC electrode and 14.00 mm^2 for the Au electrode. A platinized Pt electrode was used as the auxiliary electrode. A saturated calomel electrode (SCE) served as the reference electrode and all the potentials were reported with respect to the SCE.

Before use, the GC or Au electrode was sequentially polished with 1.0, 0.3 and 0.5 μm alumina/water slurries until a shiny, mirror-like finish was obtained. The electrode was then sonicated in triple distilled water. To prepare the Au/GC electrode, Au microparticles were electrochemically deposited on the surface of the GC electrode. The quantity of the

*Author to whom correspondence should be sent.

electrochemically deposited Au microparticles, M in $\mu g\,cm^{-2}$, was controlled and measured by concurrently measuring the charge passed for variable times by the single potential step method. Then, an ageing treatment was applied to the electrode to stabilize the Au microparticles before the electrocatalytic measurements. In the treatment, continuous potential cycling between −0.20 V and +1.45 V at a potential scanning rate of 0.5 V s^{-1} for 10 min in the 0.005 м H_2SO_4 solution was carried out.

The surface distribution of Au microparticles on the surface of the GC electrode was examined by scanning electron microscopy (model S-520, Hitachi, Japan).

3. Results and discussion

3.1. *Electrochemical deposition of Au microparticles on the surface of the GC electrode*

Figure 1(a) shows the linear sweep voltammograms at the bare GC electrode in the 5 мм $HAuCl_4$ + 0.5 м HCl + 0.25 м H_2SO_4 solution from 0.80 to –0.20 V at different scan rates. A single reduction peak at about 0.34 V is observed. The peak current, I_p is proportional to the square root of scan rate, v (Fig. 1(b)) indicating that the electrochemical reduction reaction of Au^{3+}/Au is diffusion controlled. The diffusion coefficient of $AuCl_4^-$ is 8.70×10^{-5} cm^2 s^{-1} calculated form the linear slope of the I_p against $v^{1/2}$ curve, as shown in Fig. 1(b).

Figure 2 shows the I/t transient curves in response to single potential steps from 0.80 V to different potentials. It can be seen in Fig. 2 that for each curve, the current rapidly increases and then decays to a limiting value within the first 5 s. Therefore, only the I/t curves for the first 5 s are shown in Fig. 2, although one potential step lasts for 90 s in the experiments. This kind of curve is characteristic of the formation of microcrystallities during the deposition process. The current is linearly proportional to the reciprocal of the square root of time for the decay part of the I/t transient curves (Fig. 3), indicating that Au^{3+}/Au reduction is controlled by diffusion. The diffusion coefficient of $AuCl_4^-$ calculated from the plot in Fig. 3 by means of the Cottrell equation is 8.78×10^{-5} cm^2 s^{-1}. This is in good agreement with the results from the linear sweep voltammograms.

The types of the nucleation and growth mechanisms can be distinguished by analysis of the I/t transient curves [1, 8, 17–19]. The theoretical current transients for three-dimensional nucleation with diffusion controlled growth can be described by the following equations [17, 18]:
For instantaneous nucleation,

$$I = \frac{nFD^{1/2}C}{(\pi t)^{1/2}}[1 - \exp(-\pi NkDt)] \qquad (1)$$

and for progressive nucleation,

$$I = \frac{nFD^{1/2}C}{(\pi t)^{1/2}}[1 - \exp(-AN_\infty \pi k' t^2/2)] \qquad (2)$$

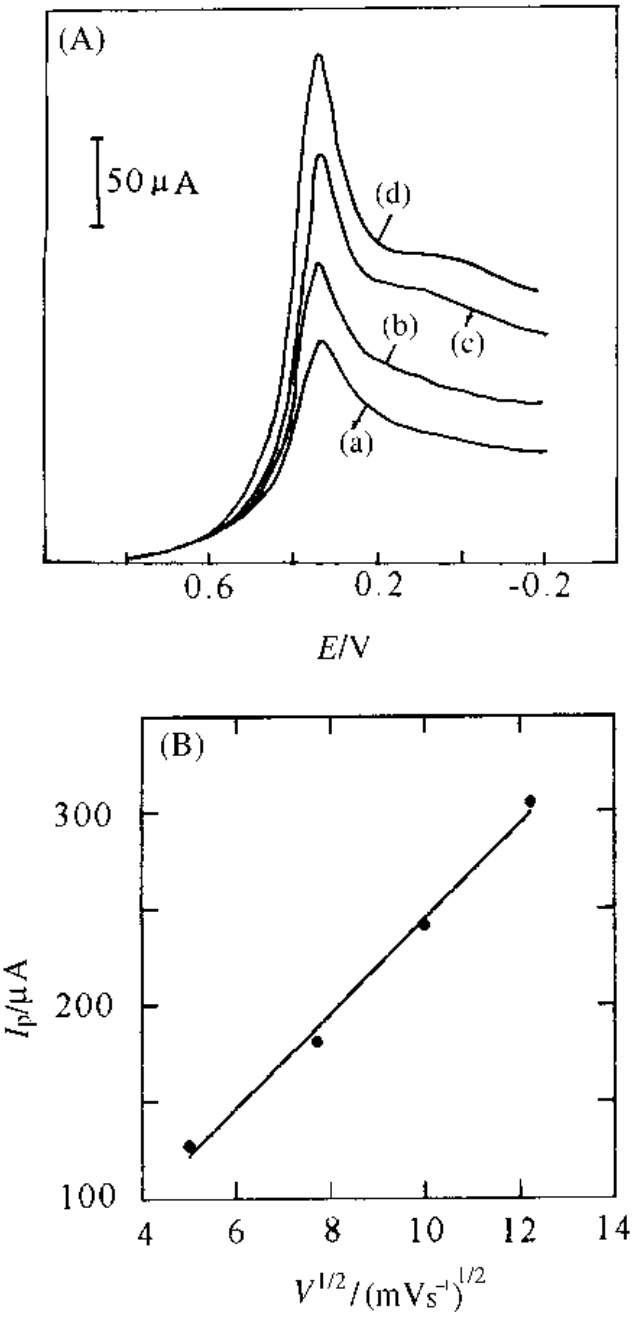

Fig. 1. (A) Linear sweep voltammograms of 5 мм $HAuCl_4$ in the 0.25 м H_2SO_4 + 0.5 м HCl solution at the GC electrode for different scan rates: (a) 25, (b) 50, (c) 100 and (d) 150 mV s^{-1}. (B) $I_p \sim v^{1/2}$ curve.

where: nF is the molar charge of the electrodeposition species; D is the diffusion coefficient; C is the bulk concentration of the active species; N is the number of nuclei per cm^2 distributed on the electrode surface; k is the constant related to the density and molar mass of the depositing species; A is the rate constant of steady state nucleation per site; N_∞ is the number density of active sites; and $k' = 4/3$ k.

Comparing the experimental I/t transient curves with the data predicted from the above models, the nucleation modes can be evaluated. In addition, the nucleation modes can also be distinguished by comparing the maximum current, I_m, and corresponding time, t_m, obtained from the I/t transient curves with

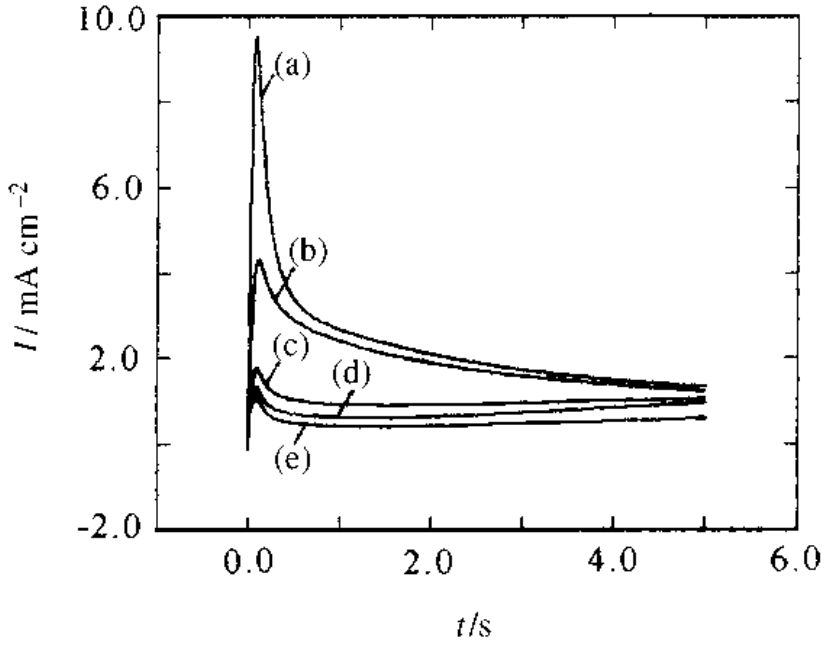

Fig. 2. *I*/*t* curves in response to single potential steps from 0.80 V to (a) 0.30, (b) 0.35, (c) 0.40, (d) 0.43 and (e) 0.45 V at the GC electrode in the 5 mM $HAuCl_4$ + 0.25 M H_2SO_4 + 0.5 M HCl solution.

that predicted from the above models. I_m and t_m can be evaluated from the first derivation of Equations 1 and 2:

For instantaneous nucleation,

$$I_m = 0.6382\ nFDC(KN)^{1/2} \quad (3)$$

$$t_m = 1.2564/n\pi kD \quad (4)$$

For progressive nucleation,

$$I_m = 0.4615\ nFD^{3/4}\,C(K'AN_\infty)^{1/4} \quad (5)$$

$$t_m = (4.6733/AN_\infty\pi k')^{1/2} \quad (6)$$

For convenience, nucleation modes can be diagnosed by comparing theoretical nondimensional $I^2/I_m{}^2$ against t/t_m plots with the experimental data [17–20]. In nondimensional forms, Equations 1 and 2 become: for instantaneous nucleation,

$$\frac{I^2}{I_m^2} = 1.9542\left\{1-\exp\left[-1.2564\left(\frac{t}{t_m}\right)\right]\right\}^2 \Big/ \left(\frac{t}{t_m}\right) \quad (7)$$

and for progressive nucleation

$$\frac{I^2}{I_m^2} = 1.2254\left\{1-\exp\left[-2.3367\left(\frac{t}{t_m}\right)^2\right]\right\}^2 \Big/ \left(\frac{t}{t_m}\right) \quad (8)$$

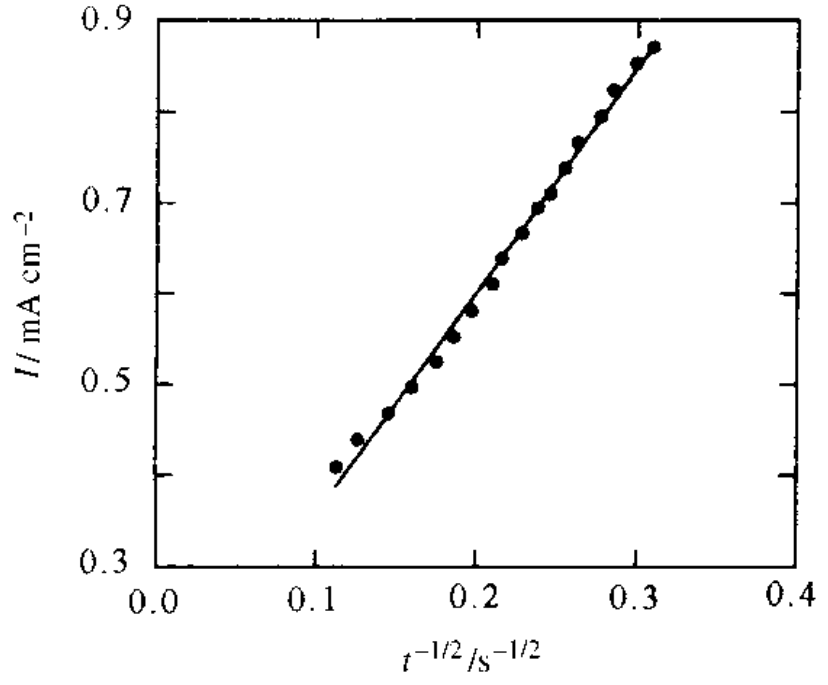

Fig. 3. $I/t^{-1/2}$ curve of the decaying portion of the transient curve (d) in Fig. 2.

Because the $I^2/I_m^2 \sim t/t_m$ relations contain no parameters which cannot be readily evaluated, such comparison is a convenient diagnostic criterion of the nucleation models.

Figure 4 shows the theoretically predicted nondimensional $I^2/I_m^2 \sim t/t_m$ curves for both instantaneous nucleation (Fig. 4, curve (a)) and progressive nucleation (Fig. 4, curve (b)) under diffusion controlled three dimension growth and a typical experimental curve (Fig. 4, curve (c)). It can be seen that the experimental data agree well with the theoretical curve for instantaneous nucleation. Therefore, the results suggest that the formation mechanism of Au microparticles on the GC electrode surface corresponds to an instantaneous nucleation and diffusion controlled three dimension growth.

3.2. *Distribution of Au particles on the GC electrode surface*

Single potential step chronoamperometry was carried out by stepping the potential of the GC electrode from 0.80 to 0.43 V at variable times and concurrently measuring the charge passed to estimate the amount of Au electrochemically deposited on the GC electrode surface, M. After the electrode had undergone an electrochemical ageing treatment, the SEM micrograph (Fig. 5) of the Au/GC electrode surface was obtained. The small, round-shaped, white spots are the Au microparticles. The figure is similar to that represented by Scharifker *et al.* [21], indicating that the distribution of the Au microparticles on the GC electrode surface is uniform. In addition, Scharifker *et al.* [21] indicated that at low overpotentials, nuclei were found to be uniformly distributed on the electrode surface. The formal potential of $AuCl_4^- + 3e^- = Au + 4Cl^-$ is 0.75 V [22]. The deposition potential of Au is 0.43 V here. Thus, the overpotential of deposition of Au is relatively low and uniformly distributed Au microparticles can be obtained on the electrode surface. The particle size was measured to be about 80 ~ 90 nm in diameter.

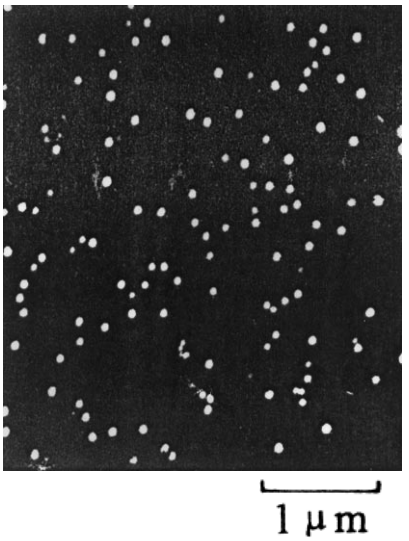

Fig. 5. SEM of an Au/GC electrode after electrochemical ageing treatment ($M = 6.08$ μg cm^{-2}).

3.3. *Electrocatalysis of Au microparticles in the oxidation of formaldehyde*

It is well known that the electrocatalytic activities of highly dispersed metal microparticles are related to the surface areas for many chemical reactions. Thus,

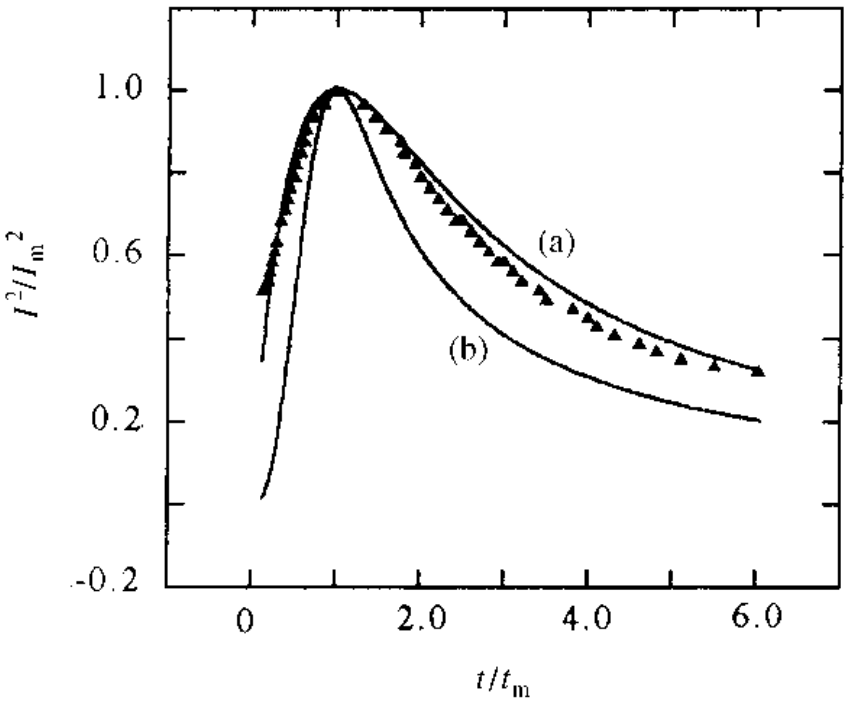

Fig. 4. Nondimensional I^2/I_m^2 against t/t_m curves for (a) instantaneous and (b) progressive nucleation models. ▲: experimental data from Fig. 2.

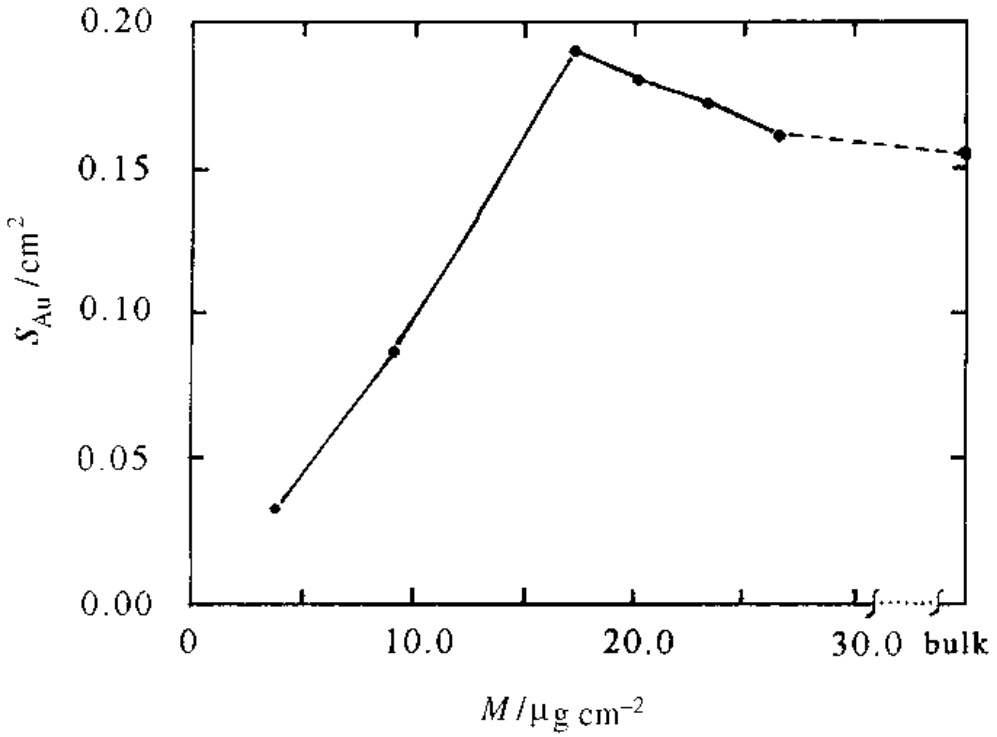

Fig. 6. Change in the real areas S_{Au} of the Au/GC and Au electrodes with the amount of electrochemically deposited Au(M).

the measurment of the real surface area was carried out after the ageing treatment of the Au/GC electrode. The real surface areas, S_{Au} can be estimated from the reduction charge of the monolayer oxides in the solution [6, 8, 23]. Figure 6 shows the dependence of S_{Au} with M. It can be seen that S_{Au} increases to a maximum and then decreases slowly with increase in M and S_{Au} for Au microparticles is higher than that for the bulk-form Au.

Typical cyclic voltammograms of 0.1 M HCHO in the 0.1 M Na_2CO_3 + 0.1 M $NaHCO_3$ solution at the Au/GC electrode (M = 20.2 μg cm^{-2} and the bulk-form Au electrode are shown in Fig. 7. The peak potential for the Au/GC electrode is about 0.14 V less

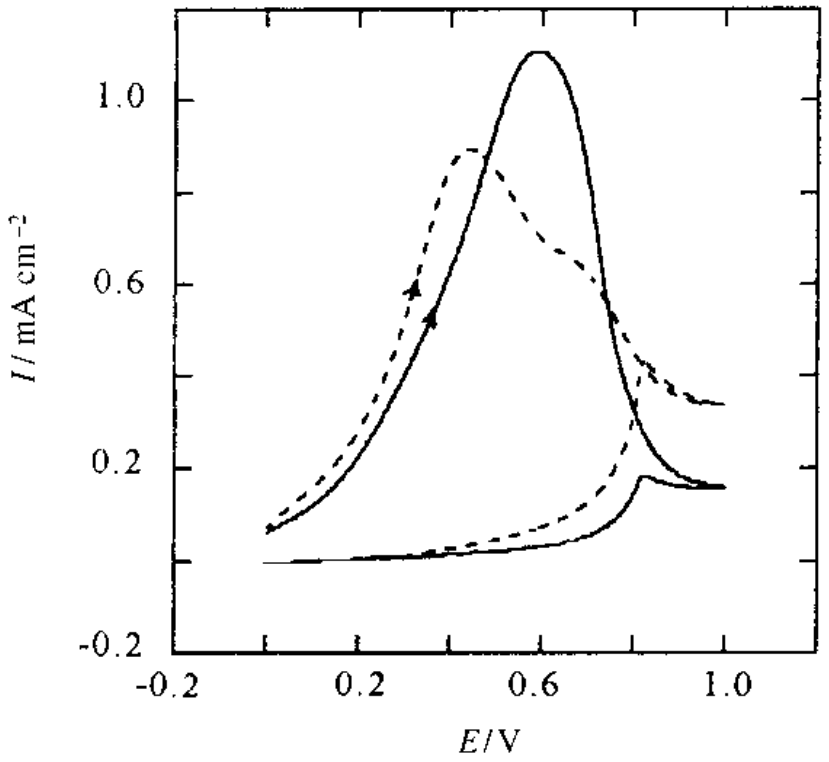

Fig. 7. Typical voltammograms of formaldehyde at the Au/GC electrode for M = 20.2 μg cm^{-2} (dotted line) and the bulk Au electrode (solid line) in the 0.1 M HCHO + 0.1 Na_2CO_3 + 0.1 M $NaHCO_3$ solution. Scan rate: 100 mV s^{-1}.

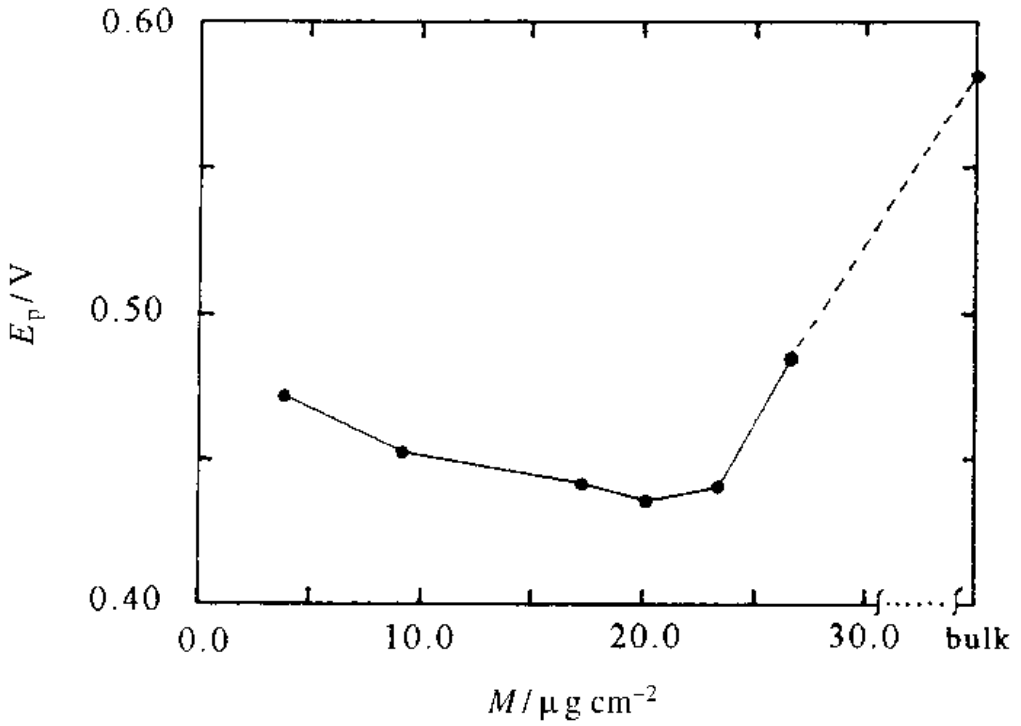

Fig. 8. Change in anodic peak potential (E_p) in the cyclic voltammograms of formaldehyde at Au/GC electrodes with M.

positive than that for the bulk-form Au electrode. Figure 8 shows the dependence of the peak potential on M. Obviously, the peak potentials at all the Au/GC electrodes are less positive than that at the bulk-form Au electrode. It can be seen that the electrocatalytic activity of the Au/GC electrodes for the electrochemical oxidation of formaldehyde increases to a maximum and then decreases with increase in M. This may be attributed to the aggregation of the Au particles with increase in M.

It can be concluded that the electrocatalytic activities for the Au/GC electrodes are better than that of the bulk form Au electrode. Further study shows that the mechanisms of the electrochemical oxidation of formaldehyde at the Au/GC electrodes are somewhat different from that at the bulk-form Au electrode. The study of the probable mechanisms of formaldehyde oxidation at the Au/GC electrodes using *in situ* FTIR and surface structural analysis techniques will be reported in a further paper.

Acknowledgement

The authors are grateful for the financial support of the State Key Laboratory for Physical Chemistry of the Solid Surface, Xiamen University, P. R. China.

References

[1] L. C. Jiang and D. Pletcher, *J. Electroanal. Chem.* **149** (1983) 237.
[2] K. Shiuaza, D. Weisshaar and T. Kuzawa, *J. Electroanal. Chem.*, **223** (1987) 223.
[3] K. Shiuaza, K. Uosaki and H. Kita, *J.Electroanal. Chem.* **256** (1988) 481.
[4] L. Nicolas and T. Kuwana, *J.Am. Chem. Soc.* **114** (1992) 769, and cited therein.
[5] K. Yahikazawa, Y. Fujii, Y. Matsuda, K. Nishimura and Y. Takasu, *Electrochim. Acta* **36** (1991) 973.
[6] N. Tateishi, K. Yahikazawa, K. Nishimura, M. Suzuki, Y. Iwanaga, M. Watanabe, E. Enami, Y. Matsuda and Y. Takasu, *ibid.* **36** (1991) 1235.
[7] N. Tateishi, K. Nishimura, K. Yahikazawa, M. Nakagawa, M. Yamada and Y. Takasu, *J.Electroanal. Chem.* **352** (1993) 243.
[8] L. Borou, M. Eyraud and J. Crousier, *J. Appl. Electrochem.* **24** (1994) 906.
[9] K. Yahikazawa, K. Nishimura, M. Kumazawa, N. Tateisha, Y. Takasu, K. Yasuda and Y. Matsuda, *Electrochim. Acta* **37** (1992) 453.
[10] B. B. Maria, *ibid.* **30** (1992) 1193.
[11] L. D. Burke, W. A. O'Leary, *J. Appl.Electrochem.* **19** (1989) 758.
[12] M. L. Avramov-Ivic, R. R. Adzic, A. Bewick and M. Razaq, *J.Electroanal. Chem.* **240** (1988) 161.
[13] M. L. Avramov-Ivic, N. Anastasijevic and R. R. Adzic *Electrochim. Acta* **35** (1990) 725.
[14] L. D. Burke and K. J. O. Dwyer, *ibid.* **35** (1990) 1829.
[15] H. Kita and H. Nakajima, *J. Electroanal. Chem.* **190** (1985) 140.
[16] L. D. Burke and V. J. Cunnane, *ibid.* **210** (1986) 69.
[17] B. Scharifker and G. Hills, *Electrochim. Acta* **28** (1983) 879.
[18] E. Bosco and S. K. Rangarajan, *J. Electroanal. Chem.* **134** (1981) 213.
[19] G. A. Gunawardena, G. J. Hills and I. Montenegro, *Electrochim. Acta*, **23** (1977) 693.
[20] S. J. Xia and W. F. Zhou, *J. Electroanal. Chem.*, **379** (1994) 361.
[21] A. Serruya, J. Mostany and R. Scharifker, *J. Chem. Soc. Faraday Trans.* **89** (1993) 255.
[22] J. Pouradier, M.C. Gadet and H.Chateau, *J.Chim. Phys.* **62** (1965) 203.
[23] D. A. J. Rand and R. Woods, *J. Electroanal. Chem.* **31** (1971) 29.